# Highly Selective Off–On Fluorescent Probe for Imaging Thioredoxin Reductase in Living Cells

Liangwei Zhang, Dongzhu Duan, Yaping Liu, Chunpo Ge, Xuemei Cui, Jinyu Sun, and Jianguo Fang*

State Key Laboratory of Applied Organic Chemistry and College of Chemistry and Chemical Engineering, Lanzhou University, Lanzhou, Gansu 730000, China

S *Supporting Information*

ABSTRACT: The first fluorescent probe for mammalian thioredoxin reductase (TrxR), TRFS-green, was designed, synthesized, and fully evaluated. The probe features a 1,2-dithiolane scaffold with a quenched naphthalimide fluorophore. TRFS-green displays a green fluorescence off–on change induced by the TrxR-mediated disulfide cleavage and subsequent intramolecular cyclization to liberate the masked naphthalimide fluorophore. It was demonstrated in vitro that TRFS-green manifests high selectivity toward TrxR over other related enzymes and various small molecule thiols as well as biological reducing molecules. HPLC analyses indicated that

TRFS-green was exclusively converted to naphthalimide catalyzed by TrxR. The ability in triggering on the fluorescence signal by cellular protein extracts correlates well with the endogenous TrxR activity in different cells. Furthermore, inhibition of TrxR by 2,4-dinitrochlorobenzene or depletion of TrxR by immunoprecipitation remarkably decreases the reduction of TRFS-green by cellular protein extracts. Finally, TRFS-green was successfully applied in imaging TrxR activity in living cells. The fluorescence signal of TRFS-green in living cells was inhibited by pretreating the cells with TrxR inhibitor in a dose-dependent manner, potentiating the development of living cell-based screening assay for identifying TrxR inhibitors. We expect the novel fluorescent probe TRFS-green would facilitate the discovery of TrxR-targeting small molecules for potential therapeutic agents and provide significant advances in understanding the physiological/pathophysiological functions of TrxR in vivo.
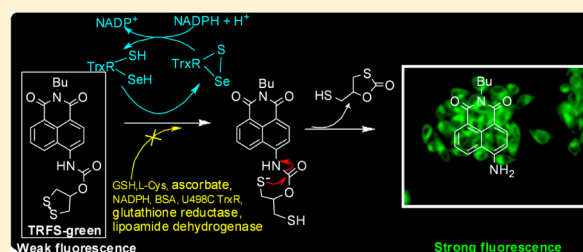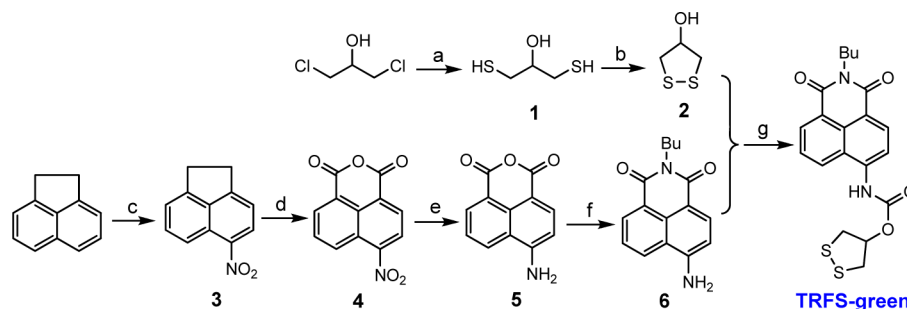
■ INTRODUCTION

Exploring biological events is critically contingent upon the development of novel assay techniques. Among the numerous detection methods, fluorescence sensing, due to its high sensitivity, operational simplicity, and biocompatibility, is one of the most powerful and popular tools to visualize the complicated biological processes.[1,2] Thus, the past decades have witnessed a burst of interests in development of diverse fluorescent probes for detection of biological molecules, such as enzymes,[3–11] metal ions,[12–15] small molecule thiols,[16–19] and reactive oxygen/nitrogen species.[20–24] Intracellular thiols, such as cysteine (Cys), glutathione (GSH), and protein thiols, play vital roles in regulating the redox-related signaling pathways and maintaining higher-order structures of proteins mainly through the equilibrium between thiols (RSH) and disulfides (RSSR).[25,26] Perturbation of the intracellular thiol-disulfide equilibrium (redox homeostasis) is tightly associated with a variety of human diseases, such as cancer, cardiovascular diseases, and neurodegenerative diseases.[27–29] Based on the unique chemical reactivity of thiols (nucleophilicity, reducing capacity, and metal ions binding property), numerous thiol-responsive fluorescent probes have been rationally developed in recent years.[17–19] Besides the small molecule thiols, a majority of redox enzymes, such as thioredoxin reductase (TrxR), glutathione reductase (GR), and methionine sulfoxide reductase, employ Cys as active residues in catalyzing reactions and

regulate the intracellular redox homeostasis. However, due to the presence of much abundant small molecule thiols, the specific reporter substrates for these enzymes in living cells are quite limited.

The thioredoxin system, composed of TrxR, thioredoxin (Trx), and NADPH, is a highly conserved network in all cells and plays a crucial role in maintaining the intracellular redox homeostasis and regulating the diverse cellular redox signaling events.[30,31] TrxR passes the electrons from NADPH to the oxidized Trx, yielding the reduced Trx, which interacts with multiple downstream proteins via a general thiol–disulfide exchange reaction. As TrxR is the only known physiological reductase of Trx, the function of the thioredoxin system is entirely dependent on the activity of TrxR. Mammalian TrxRs are homodimer selenoproteins containing a unique catalytically active selenolthiol/selenenylsulfide in the conserved C-terminal sequence -Gly-Cys-Sec-Gly.[32,33] Upon reduction, this C-terminal catalytic motif is exposed on the surface of the enzyme and easily accessed by a variety of small molecules. The presence of highly reactive selenocysteine (Sec) residue and its easy accessibility render mammalian TrxRs having a broad substrate scope and prone to be inactivated by various electrophiles.[31,34–38] TrxR is often overexpressed in many

Scheme 1. Synthesis of TRFS-Green[a]

[a](a) Na$_2$CS$_3$, 60 °C, 59%; (b) I$_2$/NaHCO$_3$/CH$_2$Cl$_2$, rt, 89%; (c) AcOH/HNO$_3$, rt, 63%; (d) Na$_2$Cr$_2$O$_7$/AcOH, reflux, 76%; (e) SnCl$_2$·2H$_2$O/HCl/EtOH, reflux; (f) C$_4$H$_9$NH$_2$/EtOH, reflux, 67% (in two steps); (g) triphosgene/DIPEA/toluene, 32%.

cancer cells and targeting its ablation leads to a reversal in the growth of numerous malignant tumors, potentiating this selenoenzyme as a promising target for development of novel anticancer agents.[30,31,34,39−41] The classic TrxR activity assays have been well developed with respect to different sources of enzyme. The purified TrxR activity is routinely determined by the 5,5′-dithiobis(2-nitrobenzoic acid) (DTNB) reduction assay, which was initially developed by Holmgren.[42] However, detection of TrxR activity in cells is time and labor consuming. Prior to the assay, cells have to be broken to extract the intracellular proteins. The activity of TrxR in cell extracts is then determined by the DTNB reduction assay coupled with addition of specific TrxR inhibitors or by the Trx-mediated insulin reduction assay.[35,36,43] To the best of our knowledge, there is no convenient and direct method in reading out the enzyme activity in living cells, and thus it limits the investigation of this pivotal redox enzyme. Herein, we first described the design, synthesis, and evaluation of a TrxR fluorogenic substrate (TRFS-green, Scheme 1). The key structure of TRFS-green is that it contains a five-membered, cyclic disulfide scaffold, which can be selectively cleaved by TrxR in the presence of NADPH. The naphthalimide moiety provides a suitable fluorescent readout because of its outstanding spectroscopic characteristics. After reducing the disulfide bond to liberate the nucleophilic thiolate, an intramolecular cyclization reaction takes place driven by the formation of a five-membered cyclic carbamate, which simultaneously releases the quenched fluorophore naphthalimide to trigger on the green fluorescent signal (Scheme 2). Various assays have been employed to demonstrate that TRFS-green displays high selectivity toward TrxR over other related enzymes, small molecule thiols, and biological reducing agents. Finally, the probe was successfully applied in imaging TrxR activity in living cells. Quantification of the fluorescence

intensity in living cells indicated that the emission signal gradually declined by pretreating the cells with increasing concentrations of TrxR inhibitor, 2,4-dinitrochlorobenzene (DNCB). Thus, the novel fluorescent probe TRFS-green would facilitate the discovery of small molecules that target TrxR as potential therapeutic agents and provide significant advances in understanding the physiological/pathophysiological functions of TrxR and the redox-related signaling pathways in vivo.

■ RESULTS AND DISCUSSION

Synthesis of TRFS-Green. TRFS-green was prepared by the synthetic routes outlined in Scheme 1. The fluorophore naphthalimide **6** was synthesized in 4 steps with the overall yield of 37% from the readily available acenaphthene by adapting the published procedures.[44−46] The TrxR-recognizing part, 1,2-dithiolan-4-ol (**2**), was synthesized in 2 steps with the overall yield of 52% from the commercially available 1,3-dichloropropan-2-ol by following previously published procedures.[47,48] For the synthesis of TRFS-green, **6** was reacted with triphosgene in the presence of N,N-diisopropylethylamine (DIPEA) in toluene, followed by the dropwise addition of **2**.[49] After purification by silica gel column chromatography, TRFS-green was obtained in 32% yield. The chemical structures of TRFS-green and the synthetic intermediates were fully characterized by ^{1}H NMR, ^{13}C NMR, EI-MS, and ESI-MS.

Fluorescence Response of TRFS-Green Toward TrxR. Initially, we determined if TRFS-green could be reduced by TrxR. TRFS-green has the maximum absorbance at around 373 nm ($\varepsilon = 8843$ M^{-1} cm^{-1}, in TE buffer). After reduction by TrxR and NADPH under the simulated physiological conditions, i.e., at 37 °C in 50 mM Tris and 1 mM EDTA (TE) buffer, pH 7.4, its maximum absorbance is red-shifted to ∼438 nm ($\varepsilon = 9936$ M^{-1} cm^{-1}, Figure 1a), and a green emission band centered at ∼538 nm appeared concomitantly (Figure 1b) when excited at 438 nm ($\phi = 0.174$ in TE buffer), whereas there is only marginal emission for TRFS-green when excited at 438 nm. TRFS-green itself emits at ∼480 nm when excited at 377 nm ($\phi = 0.178$ in TE buffer, Figure S5). The increment of fluorescence intensity is dependent on the incubation time (Figure 1c). The fluorescence emission intensity at various TrxR concentrations (0−200 nM) was also determined and shown in Figure 1d, which clearly displays a manner of TrxR concentration dependence. Absence of NADPH in the reaction mixture gives no increment of fluorescence (data not shown). It is worth noting that if the

Scheme 2. Proposed Mechanism of the Fluorescence Turn On of TRFS-Green Switched by TrxR/NADPH

TRFS-green
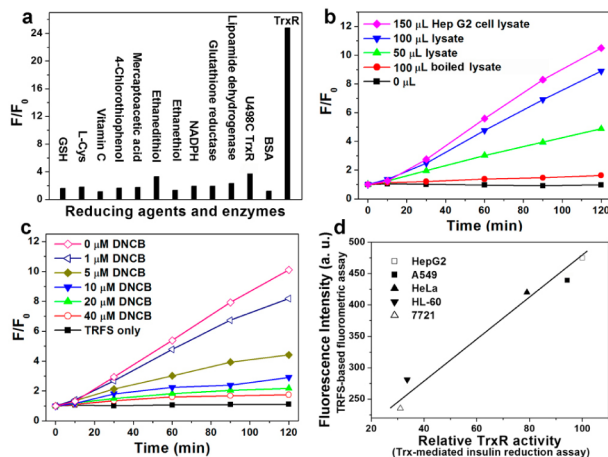Weak fluorescence

Strong fluorescence
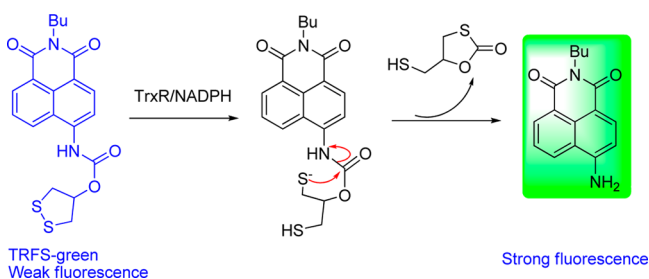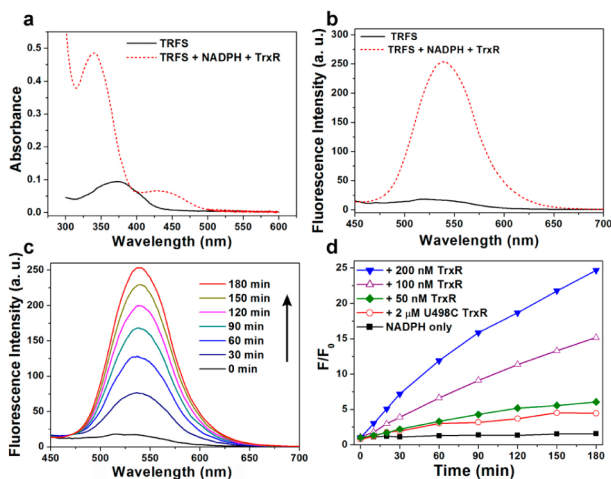
Figure 1. Spectral changes of TRFS-green during its reaction with TrxR/NADPH in TE buffer. (a) UV−vis absorption and (b) fluorescence spectra of TRFS-green (10 μM) in the absence (solid lines) and presence (dashed lines) of TrxR (75 nM) and NADPH (200 μM). The spectra were acquired 3 h after the addition of TrxR/NADPH at 37 °C. The strong absorbance at ~340 nm in Figure (a) was from NADPH. (c) Time course of fluorescence changes of TRFS-green (10 μM) in the presence of TrxR (75 nM) and NADPH (200 μM). (d) Time course of the fold of fluorescence increment (538 nm) of TRFS-green (10 μM) with various concentrations of TrxR and U498C TrxR in the presence of NADPH (200 μM). All fluorescence spectra were obtained with the excitation at 438 nm, and all the reaction mixtures contain 0.5% (v/v) of methanol.

Figure 2. (a) Fluorescence response of TRFS-green (10 μM) in the presence of TrxR/NADPH and other relevant reducing agents and enzymes. One mM for GSH, L-Cys, vitamin C, 4-chlorothiolphenol, mercaptoacetic acid, ethanedithiol, ethanethiol; 200 μM for NADPH; 20 μg/mL for glutathione reductase, lipoamide dehydrogenase; 500 μg/mL for U498C TrxR, BSA; and 11 μg/mL (200 nM) for TrxR (with 200 μM NADPH). After TRFS-green was incubated with different analytes at 37 °C for 3 h, the fold of fluorescence increment (538 nm) of TRFS-green was determined with the excitation at 438 nm, and all the reaction mixtures contain 1% (v/v) of methanol. (b) Time-dependent fluorescence response of TRFS-green (10 μM) in the presence of different amount of Hep G2 cell lysate. All reactions contain additional NADPH (200 μM), and the final volume was adjusted to 1.0 mL with TE buffer. The total protein concentration of the lysate is 2.36 mg/mL determined by the Bradford procedure using BSA as a standard, and all the reaction mixtures contain 0.5% (v/v) of methanol. (c) Inhibition of Hep G2 cell lysate-mediated TRFS-green reduction by TrxR inhibitor DNCB. The NADPH-prereduced Hep G2 cell lysate was incubated with increasing concentrations of DNCB at room temperature for 30 min, and further incubation with TRFS-green (10 μM) and NADPH (200 μM) for additional 2 h. The fold of fluorescence increment of TRFS-green was determined with the excitation at 438 nm. All the reaction mixtures contain 1% (v/v) of methanol. (d) Correlation between the TRFS-green-based and the classic TrxR activity assays (end point insulin reduction assay) of various cell lystaes. The horizontal axis indicates the relative TrxR activity in different cells determined by the end point insulin reduction assay. Hep G2 cell lysate displays the highest TrxR activity among all the tested lystaes. Thus, the TrxR activity of Hep G2 cell lysate was set as 100, and TrxR activity in other lysates was expressed as the relativity of the value. The vertical axis shows the relative fluorescence intensity of TRFS-green triggered by different cell lysates in the presence of NADPH (200 μM). All the reaction mixtures contain 1% (v/v) of methanol.

wild TrxR was replaced by the U498C mutant enzyme (U498C TrxR, the Sec in the enzyme was replaced by Cys), the increment of emission signal was sharply inhibited, demonstrating the critical role of the Sec in triggering on the fluorescence signal.

Based on the mechanism of a number of thiol-response probes, we reasoned that the spectral change was initiated by the cleavage of the disulfide bond in TRFS-green by TrxR, followed by an intramolecular attack on the amide carbonyl carbon by the nascent thiolate, yielding a five-membered cyclic carbamate and the fluorescent product naphthalimide **6** (Scheme 2). To confirm this process, we analyzed the reaction mixture by HPLC. When incubation of TRFS-green (10 μM) with TrxR (100 nM) and NADPH (200 μM) in TE buffer for 3 h at 37 °C, the desiring naphthalimide **6** is the only product in the reaction mixture with ~40% conversion based on TRFS-green (Table S1 and Figure S6). At the time point of analysis, the remaining TRFS-green (6.1 μM) plus the product **6** (4.0 μM) almost equals to the amount of starting TRFS-green (10 μM), demonstrating that TRFS-green was exclusively converted to naphthalimide **6** catalyzed by TrxR. We estimated that the conversion of TRFS-green could achieve >60% if incubating the probe with 200 nM TrxR for 3 h based on the fluorescence response curve shown in Figure 1d.

Selective Reduction of TRFS-Green by TrxR. Since the TRFS-green fluorescence signal is unambiguously switched on by TrxR in vitro, we next determined if TRFS-green could be selectively reduced by TrxR. A panel of small molecule reducing agents and related enzymes was chosen to evaluate their possible interactions with TRFS-green. As shown in Figure 2a, none of the tested small molecule reducing agents (1 mM) causes significant increment of fluorescence signal. Glutathione reductase and lipoamide dehydrogenase, whose structures are

closely related to TrxR,[50] also have little effect on the reduction of TRFS-green in the presence of NADPH. Bovine serum albumin (BSA, 0.5 mg/mL) and U498C TrxR (0.5 mg/mL), which were used to mimic the celluar proteins containing monothiol and vicinal dithiol, respectively, display negligible interference of the emission signal. DL-Dithiothreitol (DTT) and tris(2-caroxy- thyl)phosphine (TCEP) are two artificial reducing agents that are widely used in reducing disulfides. TRFS-green shows little response toward DTT at concentrations lower than 50 μM (Figure S7a). TCEP is more efficient in cleaving disulfide bond than DTT. As expected, it remarkably turns on the fluorescence at the concentration as low as 10 μM (Figure S7b). However, both DTT and TCEP are not physiologically present within mammalian systems. Thus, triggering on the TRFS-green by these artificial reducing

agents should not prevent the practical application of TRFS-green. We next turned to determine if the fluorescence signal of TRFS-green could be awaked by TrxR from cellular protein extracts. As shown in Figure 2b, total protein extracts from Hep G2 cells time- and dose-dependently trigger on the emission signal. As a control, the boiled sample has trivial effect, indicating the reduction of TRFS-green is an enzyme-catalyzed process. The reduction of TRFS-green by Hep G2 cell extract is inhibited by DNCB, a widely used inhibitor of TrxR,[37] suggesting involvement of TrxR in TRFS-green reduction by the cell lysate (Figure 2c). More interestingly, the ability of different cell lysates to turn on the fluorescence signal of TRFS-green correlates very well with the TrxR activity in the cells determined by the classic Trx-mediated insulin reduction assay (Figure 2d), strongly supporting the highly selective reduction of TRFS-green by TrxR. To further demonstrate the specific reduction of TRFS-green by TrxR, we determined the reduction of TRFS-green by Hep G2 cell lysates before and after immuno-removal of TrxR1 by a specific antibody against TrxR1. The removal of TrxR1 from the lysate remarkably reduced the fluorescence intensity ($\sim$35% decline, Figure 3a).
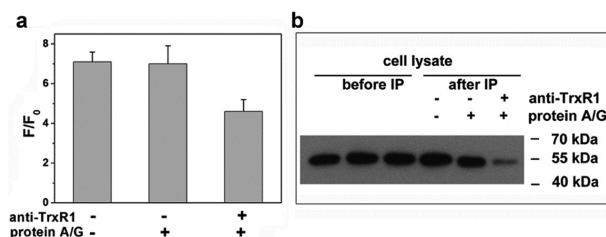

Figure 3. (a) Effect of Hep G2 cell lysate in reducing TRFS-green (10 μM) by immunodepletion of TrxR1. The cell lysates before and after IP were incubated with TRFS-green (10 μM) and NADPH (200 μM) at 37 °C for 3 h, and the fold of fluorescence increment (538 nm) was determined with the excitation at 438 nm. All the reaction mixtures contain 0.5% (v/v) of methanol. Data are expressed as mean ± standard error of three experiments. (b) Analysis of the IP efficiency by Western blots.

Figure 3b shows the TrxR1 levels in the lysates before and after immunoprecipitation (IP). It was estimated that more than 80% of TrxR1 was removed from the lysate. The remaining TRFS-green reduction activity in the lysate after IP is likely contributed from TrxR2, a mitochondrion-localized TrxR

isoform,[51,52] since the TrxR1 antibody does not cross react with TrxR2. Taken together, we firmly concluded herein that TRFS-green is a specific fluorogenic substrate for TrxR.

Viewing TrxR activity in Living Cells. With the solid results in hand, we next wonder if TRFS-green could image TrxR activity in living cells. As shown in Figure 4a, there is no fluorescence in the cells without any treatment (bottom panel, left). After incubating the cells with TRFS-green (10 μM) for 4 h, the bright green fluorescence appears (bottom panel, middle). However, if the cells were treated with DNCB (40 μM) for 2 h prior to the addition of TRFS-green, the fluorescence signal was severely inhibited (bottom panel, right). These results demonstrated that TRFS-green is suitable in imaging TrxR activity in living cells. The fluorescence intensity in single cell was quantified and shown in Figure 4b. There is no obvious cytotoxicity when Hep G2 cells were treated with TRFS-green (20 μM) for 24 h (data not shown). Further analysis and quantification of the emission intensity upon the reduction of TRFS-green by living Hep G2 cells were performed by a fluorescence plate reader (Figure 4c). Incubation of TRFS-green with the cells causes a smooth increment of emission signal, indicating a time-dependent reduction of the probe by the intracellular TrxR (line with closed squares in Figure 4c). The fluorescence readout was gradually turned down when the cells were pretreated with increasing concentrations of DNCB, a cell membrane permeable TrxR inhibitor. Thus, our results potentiate the probe in the development of a living cell-based screening assay, which is expected to identify more physiologically relevant TrxR inhibitors as potential therapeutic agents.

TrxR, a pivotal enzyme in maintaining intracellular redox balance, plays key roles in regulation of cell growth, differentiation, and death. Its malfunction is critically related to a variety of diseases, such as cancer and neurodegenerative diseases.[40,53] Hence, the past decades have witnessed increasing interests in developing therapeutic molecules that target TrxR.[31,54−58] Several reliable TrxR assays have been elegantly developed and are widely applied in numerous laboratories.[43] These assays require either purified TrxR or crude protein extracts from cells or tissues, which are time and labor consuming. What's more, the assays can not provide real time information of TrxR function in living systems. We described herein for the first time that a turn-on fluorescent probe, TRFS-green, with high selectivity toward TrxR was successfully
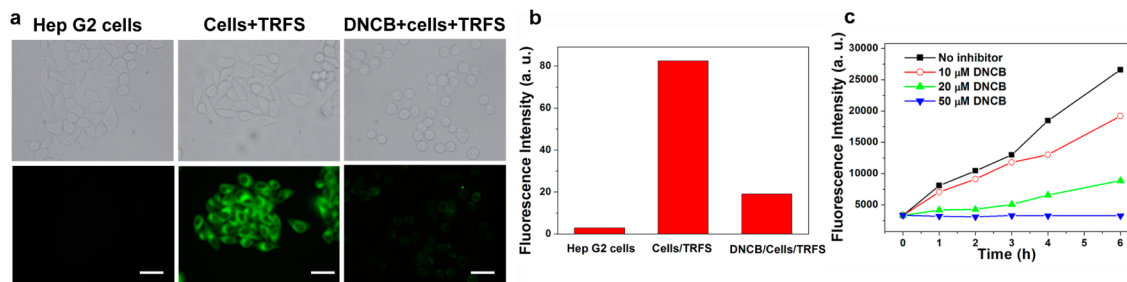
Figure 4. Fluorescence changes of TRFS-green in living Hep G2 cells. (a) Hep G2 cells only (left), Hep G2 treated with TRFS-green (10 μM) for 4 h (middle), and Hep G2 treated with DNCB (40 μM) for 2 h followed by further treated with TRFS (10 μM) for 4h (right). Scale bar: 20 μm. (b) Relative fluorescence intensity in single cell in (a) was quantified by the software of Leica Qwin accompanied with the Leica microscope. Ten cells were selected randomly, and the fluorescence intensity in individual cells was quantified. (c) Quantification of fluorescence intensity of TRFS-green in Hep G2 cells. The cells were treated with different concentrations of DNCB for 2 h and then with TRFS-green (10 μM). The fluorescence intensity in each well was read with a plate reader (excitation, 438 nm; emission, 538 nm) at the indicated time points. The final concentration of organic solvent (DMSO) in all cell culture medium is 0.5% (v/v).

prepared. The probe is suitable for living cell imaging and has potential in developing a convenient cell-based assay for TrxR inhibitor screening. We expect this novel probe will facilitate the study of TrxR function in vivo and the development of novel TrxR-targeting molecules for potential therapeutic agents.

A key feature of mammalian TrxRs different from other related enzymes is that it contains a highly reactive Sec residue at its C-terminal active site. This residue is exposed on the surface of the enzyme when TrxR is in a reduced state, which is a predominant form under physiological conditions since NADPH is usually quite abundant in cells. Due to the high reactivity and easy accessibility of the Sec residue, mammalian TrxRs can reduce diverse small molecules, including disulfide compounds. Based on the well-known mechanism of various thiol-responsive fluorescent probes,[18,19] we reasoned that if a disulfide bond could be selectively cleaved by TrxR, a specific probe to recognize the enzyme might be designed. Since linear disulfides are known to be nonselectively reduced by small molecule thiols or protein thiols,[18,19] we turned to cyclic disulfide molecules. It was reported that cyclic disulfides, such as lipoamide and lipoic acid, are substrates of TrxR[59] but can not be reduced by GSH, probably due to a much lower redox potential of the reduced lipoic acid (∼ −320−290 mv for reduced lipoic acid,[60,61] ∼ −300 mv for mammalian TrxR,[62,63] and ∼ −240 mv for GSH[64]). Thus, we chose 1,2-dithiolane as a possible TrxR-recognizing scaffold, and TRFS-green was designed, synthesized, and fully evaluated.

Fluorescent probes have multiple advantages over other techniques in exploring the complicated biological processes. However, specific recognition by the target protein is a key challenge in designing practically applicable probes. As for selective detection of TrxR within the cellular milieu, the comparatively high concentrations of biological sulfur species, such as GSH and Cys residues in proteins, are potential interference. We demonstrated here that TRFS-green is a highly selective turn-on probe for TrxR. Unlike the recently reported probe for small redox protein Trx,[11] our probe shows no response to GSH or Cys, the predominant thiols in cells, or the endogenous reducing agents, such as vitamin C and NADPH. Other related enzymes, such as glutathione reductase and lipoamide dehydrogenase, also have little effect in turning on the fluorescence signal. The mutant enzyme, U498C TrxR, gives slight increment of the emission intensity at a very high concentration, indicating the critical role of the Sec residue in switching on the fluorescence. Furthermore, the ability to reduce TRFS-green by different cell lysates correlates well with their intrinsic TrxR activity, suggesting that TrxR is a key determinant in reducing the probe. The most convincing evidence comes from the IP experiment. After immunoremoval of TrxR1 from the Hep G2 cell lysates, the fluorescence intensity was remarkably inhibited, strongly supporting the highly selective reduction of TRFS-green by TrxR.

The fluorescence intensity of TRFS-green triggered by TrxR appears keeping increase even after 3 h (Figure 1d). As evidenced by the HPLC analyses, incubation of the probe with 100 nM TrxR for 3 h, about 40% conversion achieved. Compared to the widely used, nonselective colorimetric substrate DTNB, TRFS-green displays longer response time in turning on the fluorescence signal. Perhaps this is a common drawback for the reaction-based sensors (chemodosimeters).[65] However, this drawback does not prevent the probe from practical applications in imaging TrxR, as well demonstrated in this work. According to the fluorescence turn-on mechanism

proposed in Scheme 2, there are two cascade reactions in the process of switching on the emission signal, i.e., reduction of the disulfide bond and subsequently intramolecular cyclization. We speculated that both steps might contribute to the slow response of TRFS-green under our experimental conditions. The low efficiency of reduction of TRFS-green was supported by the observation that the TrxR-recognizing scaffold, 2-dithiolan-4-ol (**2**), is a poor substrate of TrxR (K_m = 189 μM, Figure S8). Also, the second step, i.e., intramolecular cyclization, could not be favored since the amino group is not a good leaving group under neutral conditions. This is supported from the experiment that the fluorescence signal could not approach a plateau within 2 h even in the presence of 1 mM TCEP (Figure S7b), since TCEP is known to reduce disulfides very quickly and almost quantitatively. Tuning the 2-dithiolan-4-ol moiety and replacing the aminonaphthalimide in TRFS-green with other better leaving groups, such as hydroxynaphthalimide or mercaptonaphthalimide, might be promising ways in improving the response time toward TrxR.

■ CONCLUSIONS

In conclusion, TRFS-green, a turn-on fluorescent probe with high selectivity toward TrxR, was prepared and fully evaluated. The probe features a 1,2-dithiolane scaffold, the disulfide bond of which can be selectively cleaved by TrxR. Upon reduction, the nascent thiolate subsequently attacks the amide carbonyl carbon driven by forming a five-membered carbamate ring and simultaneously releasing the naphthalimide fluorophore. The probe was successfully applied in imaging the enzyme activity in living cells and has a potential application in screening TrxR inhibitors in living cells. We expect that this novel probe would be a powerful tool in understanding the physiological functions of TrxR and the cellular redox signaling events.

■ EXPERIMENTAL SECTION

Materials and Instruments. The recombinant rat TrxR1 was essentially prepared as described[66] and is a gift from Prof. Arne Holmgren at Karolinska Institute, Sweden. The recombinant U498C TrxR1 mutant (Sec→Cys) was produced as described.[67] Proteins were pure as judged by Coomassie-stained SDS-polyacrylamide gel electrophoresis (SDS-PAGE), and the recombinant TrxR1 has a specific activity of 50% of the wild TrxR1 with DTNB assay. *E. coli* Trx was purchased from IMCO (Stockholm, Sweden, www.imcocorp.se). Dulbecco's modified Eagle's medium (DMEM), bovine insulin, DTT, TCEP, GSH, DNCB, DTNB, DMSO, yeast glutathione reductase were obtained from Sigma-Aldrich (St. Louis, USA). NADPH was obtained from Roche (Mannheim, Germany). Fetal bovine serum (FBS) was obtained from Sijiqing (Hangzhou, China). Aniti-TrxR1 antibody was purchased from Santa Cruz Biotechnology (Santa Cruz, USA). 3-(4,5-dimethylthiazol-2-yl)-2,5-diphenyltetrazolium bromide (MTT), penicillin, and streptomycin were obtained from Sangon (Shanghai, China). BSA and phenylmethylsulfonyl fluoride (PMSF) were obtained from Beyotime (Nantong, China). All other reagents were of analytical grade and were purchased from commercial supplies. Absorption spectra were recorded on Multiskan GO (Thermo Scientific). Fluorescence studies were carried out using a Hitachi F-4500 fluorescence spectrofluorometer. The molar extinction coefficients (ε) and absolute quantum yields (ϕ) of TRFS-green and naphthalimide **6** were determined on UV−vis spectrometer evolution 200 (Thermo Scientific) and fluorescence spectrometer FLS920 (Edinburgh Instruments), respectively. MS spectra were recorded on Trace DSQ GC-MS spectrometer or Bruker Daltonics esquire 6000 mass spectrometer. HRMS was obtained on Orbitrap Elite (Thermo Scientific). HPLC analyses were performed on Waters 1525.

Synthesis of Compound 1.[48,68] Sodium sulfide nonahydrate (24 g, 100 mmol) was dissolved in 12 mL of water at 30 °C. To this solution

was added 8.36 g (110 mmol) of carbon disulfide. After the reaction mixture was warmed to 40 °C and allowed to stir for 6 h, the excess carbon disulfide was removed by evaporation at reduced pressure. The resulting deep red liquid was diluted by water to total volume of 46 mL to afford a ~33% solution of sodium trithiocarbonate. 1,3-Dichloro-2-propanol (4.61g, 35 mmol) was added dropwisely to the freshly prepared sodium trithiocarbonate solution at room temperature, and the reaction was kept at 60 °C for 5 h. The basic reaction mixture was acidified by sulfuric acid, and the acidic aqueous medium was extracted three times with ether (3 × 100 mL). The combined ether extract was washed with water, dried over anhydrous magnesium sulfate, and evaporated at reduced pressure to yield the crude product, which was further purified by distillation under reduced pressure to afford compound **1** as a colorless oil (2.56 g, 59%). ^{1}H NMR (400 MHz, CDCl$_3$) δ: 3.75−3.67 (m, 1H), 3.50 (d, J = 5.0 Hz, 1H), 2.81−2.67 (m, 4H), 1.47 (t, J = 8.7 Hz, 2H). ^{13}C NMR (100 MHz, CDCl$_3$) δ: 72.90, 29.83. EI-MS m/z (%): 124 (M$^+$, 8), 106 ([M − H$_2$O]$^+$, 100), 77 (46), 59 (83).

Synthesis of Compound 2.[47,68] Compound **1** (372 mg, 3 mmol) was dissolved in CH$_2$Cl$_2$ (150 mL). NaHCO$_3$ (756 mg, 9 mmol) and iodine (2.286 g, 9 mmol) were added successively to the solution. The mixture was stirred for 15 min at room temperature. The excess iodine was decomposed by addition of Na$_2$S$_2$O$_3$ (3 M in water; 110 mL). The product was extracted with CH$_2$Cl$_2$ (3 × 100 mL). The organic phase was dried over Na$_2$SO$_4$ and evaporated to dryness in vacuo. The crude product was purified by silica gel chromatography (petroleum ether/AcOEt: 50/50) to give 325 mg of compound **2** (89%) as a yellow solid. ^{1}H NMR (400 MHz, DMSO) δ: 5.28 (d, J = 4.5 Hz, 1H), 4.80−4.74 (m, 1H), 3.17 (dd, J = 11.6, 5.0 Hz, 2H), 2.98 (dd, J = 11.6, 3.2 Hz, 2H). ^{13}C NMR (100 MHz, DMSO) δ: 75.47, 46.24. EI-MS m/z (%): 122 (M$^+$, 100), 78 (51), 58 (42).

Synthesis of Compound 3.[46] To the mixture of acenaphthene (7.7g, 50 mmol) and acetic acid (60 mL) was added nitric acid (5.5 mL) with stirring at room temperature. After 4 h, the reaction mixture was poured into ice water. The precipitate was filtered and washed with water. The crude product was recrystallized from acetic acid and then ethanol to afford compound **3** (6.27g, 63% yield). ^{1}H NMR (400 MHz, CDCl$_3$) δ: 8.56 (d, J = 8.6 Hz, 1H), 8.50 (dd, J = 7.7, 2.2 Hz, 1H), 7.73 (t, J = 7.8 Hz, 1H), 7.45 (d, J = 7.0 Hz, 1H), 7.33 (d, J = 7.7 Hz, 1H), 3.48 (dd, J = 16.1, 6.7 Hz, 4H). ^{13}C NMR (100 MHz, CDCl$_3$) δ: 155.74, 146.61, 140.14, 131.98, 127.74, 124.39, 121.22, 120.13, 117.93, 30.61, 30.57. EI-MS m/z (%): 199 (M$^+$, 86), 152 (100).

Synthesis of Compound 4.[44] To a stirred solution of sodium dichromate (2.24 g, 7.5 mmol) and acetic acid (5 mL) was added the solution of compound **3** (0.60 g, 3 mmol in 5 mL acetic acid). After heating at reflux for 5 h, the reaction mixture was mixed with cold water (50 mL) at 0 °C and then filtered and washed with water until the filtrate was neutral. The residue was dried in vacuo to afford the product (0.63 g, 87% yield). ^{1}H NMR (400 MHz, DMSO) δ 8.76 (dd, J = 8.7, 0.9 Hz, 1H), 8.70−8.61 (m, 2H), 8.56 (d, J = 8.0 Hz, 1H), 8.12 (dd, J = 8.7, 7.3 Hz, 1H). ^{13}C NMR (100 MHz, DMSO) δ: 160.03, 159.43, 149.55, 133.17, 131.04, 130.58, 130.26, 129.76, 124.34, 124.09, 122.77, 120.06. EI-MS m/z (%): 243 (M$^+$, 100), 199 (66), 153 (82), 125 (61).

Synthesis of Compound 5.[44] To a stirred cloudy solution of compound **4** (120 mg, 0.5 mmol) in ethanol (5 mL) was added dropwisely the solution of SnCl$_2$·2H$_2$O (677 mg, 3 mmol) in concentrated hydrochloric acid (1 mL) at room temperature. The reaction was heated to reflux for 8 h. After cool down to room temperature, aqueous solution of Na$_2$CO$_3$ (10%) was added to quench the reaction. The precipitate was collected by filtration, washed with water (3 × 10 mL), and dried in vacuo to afford the crude product **5**, which was directly used for the preparation of compound **6** without further purification.

Synthesis of Compound 6.[45] N-butylamine (0.1 mL, 1 mmol) was quickly added to a cloudy solution of **5** (108 mg, 0.5 mmol) in ethanol (10 mL). After refluxing for 6 h, the reaction was allowed to cool to room temperature. The solvent was removed in vacuo, and the crude product was purified by silica gel column chromatography (chloro-

form/acetone: 6/1) to give 90 mg of compound **6** (67%) as a brown yellow solid. ^{1}H NMR (400 MHz, DMSO) δ 8.60 (d, J = 8.4 Hz, 1H), 8.42 (d, J = 7.1 Hz, 1H), 8.18 (d, J = 8.4 Hz, 1H), 7.65 (t, 1H), 7.44 (s, 2H), 6.83 (d, J = 8.4 Hz, 1H), 4.01 (dt, J = 12.7, 7.3 Hz, 2H), 1.57 (dt, J = 15.0, 7.5 Hz, 2H), 1.33 (dt, J = 14.9, 7.4 Hz, 2H), 0.90 (t, J = 7.3 Hz, 3H). ^{13}C NMR (100 MHz, DMSO) δ: 163.74, 162.88, 152.66, 133.90, 130.94, 129.24, 123.93, 121.79, 119.36, 108.14, 107.58, 59.75, 29.84, 19.85, 13.75. ESI-MS (m/z): [M + H]$^+$ 269.2.

Synthesis of TRFS-Green.[49] To a mixture of **6** (60 mg, 0.14 mmol) and DIPEA (67 mg, 0.52 mmol) in toluene (5 mL) was added a solution of triphosgene (52 mg, 0.17 mmol) in toluene, and the reaction was kept on ice for 1h. The resulting solution was heated to reflux for 3 h. After cooling to room temperature, the reaction mixture was diluted with CH$_2$Cl$_2$ (6 mL) and filtered. To the filtrate was added the compound **2** (22 mg, 0.18 mmol), and the solution was stirred at room temperature for an additional 3 h. The reaction mixture was concentrated, and the crude product was purified by silica gel column chromatography (1:1 EtOAc/petroleum ether) to give TRFS-green (19 mg, 32% yield). ^{1}H NMR (400 MHz, CDCl$_3$) δ 8.63 (dd, J = 15.2, 7.8 Hz, 2H), 8.35 (d, J = 8.2 Hz, 1H), 8.21 (d, J = 8.5 Hz, 1H), 7.80 (dd, J = 8.4, 7.4 Hz, 1H), 7.53 (s, 1H), 5.91 (m, 1H), 4.18 (t, 2H), 3.46 (dd, J = 12.8, 5.3 Hz, 2H), 3.39 (dd, J = 12.8, 2.5 Hz, 2H), 1.78−1.67 (m, 2H), 1.46 (dq, J = 14.8, 7.4 Hz, 2H), 0.99 (t, 3H). ^{13}C NMR (100 MHz, CDCl3) δ: 164.04, 163.56, 152.18, 138.26, 132.34, 131.31, 128.85, 126.77, 125.73, 123.48, 122.85, 118.24, 116.82, 45.08, 40.24, 30.16, 20.36, 13.84. ESI-MS (m/z): [M + H]$^+$ 417.2. HRMS (m/z): [M + Na]$^+$ calcd for 439.0762, found 439.0752 (Figure S4).

UV−vis and Fluorescence Spectroscopy. All the enzymatic reactions were performed at 37 °C in TE buffer unless otherwise stated. UV−vis spectra were acquired from Multiskan GO (Thermo Scientific). Fluorescence spectroscopic studies were performed with a Hitachi F-4500 fluorescence spectrophotometer. The slit width was 5 nm for both excitation and emission. For absorption or fluorescence measurements, compounds were dissolved in methanol, DMSO, or double distilled water to obtain stock solutions (1−10 mM). These stock solutions were diluted with TE buffer to the desired concentration. The organic solvent is no more than 1% (v/v) in all experiments.

Reduction of TRFS-Green by TrxR in Vitro and in Cell Lysates. TRFS-green (10 μM), various concentrations of TrxR, and NADPH (200 μM) were mixed in TE buffer and incubated at 37 °C. Fluorescence spectra were recorded at indicated time points. The lysates were prepared from different cells by lysing the cells with RIPA buffer (50 mM Tris-HCl pH 7.5, 2 mM EDTA, 0.5% deoxycholate, 150 mM NaCl, 1% TritonX-100, 0.1% SDS, 1 mM Na$_3$VO$_4$, and 1 mM PMSF). Total protein concentrations were quantified by the Bradford procedure using BSA as standard. To assay the ability of different cell lysates in reducing TRFS-green, additional NADPH (200 μM) was supplied. For the DNCB inhibition assay, the lystaes were prereduced with NADPH (200 μM) for 10 min and then incubated with DNCB for additional 0.5 h at room temperature.

Determination of TrxR Activity in Cells. Cells were washed twice with PBS before harvesting. Total cellular proteins were extracted by RIPA buffer for 30 min on ice. The protein content was quantified using the Bradford procedure using BSA as standard. TrxR activity in cell lysates was measured by the end point insulin reduction assay.[35,36,43] Briefly, the cell extract (20 μg of total proteins) was incubated in a final reaction volume of 50 μL containing 100 mM Tris-HCl (pH 7.4), 0.3 mM insulin, 660 μM NADPH, 3 mM EDTA, and 15 μM E. coli Trx for 30 min at 37 °C. The reaction was terminated by adding 200 μL of 1 mM DTNB in 6 M guanidine hydrochloride, pH 8.0. A blank sample, containing everything except Trx, was treated in the same manner. The absorbance at 412 nm was measured, and the blank value was subtracted from the corresponding absorbance value of the sample. Hep G2 cells have the highest TrxR activity, and TrxR activity in other cells was expressed as the percentage of the TrxR activity in Hep G2 cells.

IP and Western Blots. Hep G2 cells were lysed with RIPA buffer, and the cell lysates were diluted 5 times with PBS to obtain a solution of ~1.5 mg/mL of total proteins. The diluted cell lysates were

231

dx.doi.org/10.1021/ja408792k | *J. Am. Chem. Soc.* 2014, 136, 226−233

incubated with anti-TrxR1 antibody (Santa Cruz Biotechnology) for 2 h at room temperature and further incubated with Protein A/G-Agarose (Santa Cruz Biotechnology) for 1 h at room temperature. The agarose beads were pelleted by centrifugation (1000 g for 5 min), and the TrxR1-depleted supernatant was collected and immediately used to measure TrxR activity. For Western blot analysis, equal amounts of protein in cell lysates were separated by SDS-PAGE and electroblotted onto PVDF membranes (Millipore, USA). After blocking with 5% nonfat milk in TBST (20 mM Tris, pH 7.6, 0.14 mM NaCl, and 0.1% Tween-20) at room temperature for 2 h, the membranes were incubated with primary antibodies at 4 °C overnight. The membranes were washed with TBST for three times and further incubated with the horseradish peroxidase-conjugated secondary antibodies at room temperature for 1 h. The signal was detected using an enhanced chemiluminescence (ECL) kit from GE Healthcare.

Living Cell Imaging. Hep G2 cells were seeded in a 12-well plate and cultured in DMEM supplemented with 10% FBS, 2 mM glutamine, penicillin (100 units/mL), streptomycin (100 units/mL) at 37 °C in a humidified atmosphere of 5% CO_2 overnight. TRFS-green (10 μM) was added, and the cells were incubated for another 4 h. The cells were rinsed with the medium for three times to remove the remaining TRFS-green. To inhibit the cellular TrxR, the cells were treated with DNCB (40 μM) for 2 h prior to TRFS-green treatment. The fluorescence images were acquired by a fluorescent microscope (Leica DM 4000B microscope). The quantification of cellular fluorescence intensity was performed by a fluorescent microplate reader (TECAN Infinite M200). Hep G2 cells were plated at 10 000 cells per well in a clear bottom, black wall, 96-well plate with complete culture medium. After 24 h, the cells were treated with different concentrations of DNCB for 2 h and then with TRFS-green (10 μM). The fluorescence intensity in each well was read with the plate reader (excitation, 438 nm; emission, 538 nm) at the indicated time points.

■ ASSOCIATED CONTENT

Ⓢ Supporting Information

The NMR and MS spectra of TRFS-green, HPLC analyses of TrxR-mediated TRFS-green reduction, and other materials are available free of charge via the Internet at http://pubs.acs.org.

■ AUTHOR INFORMATION

Corresponding Author

fangjg@lzu.edu.cn

Notes

The authors declare no competing financial interest.

■ ACKNOWLEDGMENTS

■ REFERENCES

(1) *Molecular Fluorescence: Principles and Applications*; Valeur, B., Ed.; Wiley: Hoboken, NJ, 2002.

(2) *The Molecular Probes Handbook*; 11th ed.; Johnson, I., Spence, M. T. Z., Eds.; Life Technologies Corporation: Carlsbad, CA, 2010.

(3) Sakabe, M.; Asanuma, D.; Kamiya, M.; Iwatate, R. J.; Hanaoka, K.; Terai, T.; Nagano, T.; Urano, Y. *J. Am. Chem. Soc.* **2013**, *135*, 409.

(4) Silvers, W. C.; Prasai, B.; Burk, D. H.; Brown, M. L.; McCarley, R. L. *J. Am. Chem. Soc.* **2013**, *135*, 309.

(5) Myochin, T.; Hanaoka, K.; Komatsu, T.; Terai, T.; Nagano, T. *J. Am. Chem. Soc.* **2012**, *134*, 13730.

(6) Li, L.; Ge, J.; Wu, H.; Xu, Q. H.; Yao, S. Q. *J. Am. Chem. Soc.* **2012**, *134*, 12157.

(7) Chang, J. W.; Moellering, R. E.; Cravatt, B. F. *Angew. Chem., Int. Ed. Engl.* **2012**, *51*, 966.

(8) Baba, R.; Hori, Y.; Mizukami, S.; Kikuchi, K. *J. Am. Chem. Soc.* **2012**, *134*, 14310.

(9) Mizukami, S.; Takikawa, R.; Sugihara, F.; Shirakawa, M.; Kikuchi, K. *Angew. Chem., Int. Ed. Engl.* **2009**, *48*, 3641.

(10) Fujikawa, Y.; Urano, Y.; Komatsu, T.; Hanaoka, K.; Kojima, H.; Terai, T.; Inoue, H.; Nagano, T. *J. Am. Chem. Soc.* **2008**, *130*, 14533.

(11) Lee, M. H.; Han, J. H.; Lee, J. H.; Choi, H. G.; Kang, C.; Kim, J. S. *J. Am. Chem. Soc.* **2012**, *134*, 17314.

(12) Pluth, M. D.; Tomat, E.; Lippard, S. J. *Annu. Rev. Biochem.* **2011**, *80*, 333.

(13) Que, E. L.; Domaille, D. W.; Chang, C. J. *Chem Rev* **2008**, *108*, 1517.

(14) Kim, M. K.; Lim, C. S.; Hong, J. T.; Han, J. H.; Jang, H. Y.; Kim, H. M.; Cho, B. R. *Angew. Chem., Int. Ed. Engl.* **2010**, *49*, 364.

(15) Hu, R.; Feng, J.; Hu, D.; Wang, S.; Li, S.; Li, Y.; Yang, G. *Angew. Chem., Int. Ed. Engl.* **2010**, *49*, 4915.

(16) Lin, V. S.; Chang, C. J. *Curr. Opin. Chem. Biol.* **2012**, *16*, 595.

(17) Chen, X.; Zhou, Y.; Peng, X.; Yoon, J. *Chem. Soc. Rev.* **2010**, *39*, 2120.

(18) Jung, H. S.; Chen, X.; Kim, J. S.; Yoon, J. *Chem. Soc. Rev.* **2013**, *42*, 6019.

(19) Lee, M. H.; Yang, Z.; Lim, C. W.; Lee, Y. H.; Dongbang, S.; Kang, C.; Kim, J. S. *Chem. Rev.* **2013**, *113*, 5071.

(20) Yuan, L.; Lin, W.; Xie, Y.; Chen, B.; Zhu, S. *J. Am. Chem. Soc.* **2012**, *134*, 1305.

(21) Miller, E. W.; Chang, C. J. *Curr. Opin. Chem. Biol.* **2007**, *11*, 620.

(22) McQuade, L. E.; Lippard, S. J. *Curr. Opin. Chem. Biol.* **2010**, *14*, 43.

(23) Kundu, K.; Knight, S. F.; Willett, N.; Lee, S.; Taylor, W. R.; Murthy, N. *Angew. Chem., Int. Ed. Engl.* **2009**, *48*, 299.

(24) Wardman, P. *Free Radicals Biol. Med.* **2007**, *43*, 995.

(25) Bindoli, A.; Rigobello, M. P. *Antioxid. Redox Signaling* **2013**, *18*, 1557.

(26) Paulsen, C. E.; Carroll, K. S. *Chem. Rev.* **2013**, *113*, 4633.

(27) Circu, M. L.; Aw, T. Y. *Free Radicals Biol. Med.* **2010**, *48*, 749.

(28) Ueda, S.; Masutani, H.; Nakamura, H.; Tanaka, T.; Ueno, M.; Yodoi, J. *Antioxid Redox Signaling* **2002**, *4*, 405.

(29) Powis, G.; Gasdaska, J. R.; Baker, A. *Adv. Pharmacol.* **1997**, *38*, 329.

(30) Lu, J.; Holmgren, A. *Antioxid. Redox Signaling* **2012**, *17*, 1738.

(31) Cai, W.; Zhang, L.; Song, Y.; Wang, B.; Zhang, B.; Cui, X.; Hu, G.; Liu, Y.; Wu, J.; Fang, J. *Free Radicals Biol. Med.* **2012**, *52*, 257.

(32) Zhong, L.; Arner, E. S.; Holmgren, A. *Proc. Natl. Acad. Sci. U.S.A.* **2000**, *97*, 5854.

(33) Gladyshev, V. N.; Jeang, K. T.; Stadtman, T. C. *Proc. Natl. Acad. Sci. U.S.A.* **1996**, *93*, 6146.

(34) Arner, E. S. *Biochim. Biophys. Acta* **2009**, *1790*, 495.

(35) Fang, J.; Holmgren, A. *J. Am. Chem. Soc.* **2006**, *128*, 1879.

(36) Fang, J.; Lu, J.; Holmgren, A. *J. Biol. Chem.* **2005**, *280*, 25284.

(37) Nordberg, J.; Zhong, L.; Holmgren, A.; Arner, E. S. *J. Biol. Chem.* **1998**, *273*, 10835.

(38) Cai, W.; Zhang, B.; Duan, D.; Wu, J.; Fang, J. *Toxicol. Appl. Pharmacol.* **2012**, *262*, 341.

(39) Mahmood, D. F.; Abderrazak, A.; Khadija, E. H.; Simmet, T.; Rouis, M. *Antioxid. Redox Signaling* **2013**, *19*, 1266-13032013.

(40) Powis, G.; Kirkpatrick, D. L. *Curr. Opin. Pharmacol.* **2007**, *7*, 392.

(41) Holmgren, A.; Lu, J. *Biochem. Biophys. Res. Commun.* **2010**, *396*, 120.

(42) Holmgren, A. *J Biol. Chem.* **1977**, *252*, 4600.

(43) Arner, E. S.; Holmgren, A. *Curr. Protoc. Toxicol.*; Wiley: Hoboken, NJ, 2001; Chpt 7, Unit 7 4.

(44) Dong, M.; Wang, Y. W.; Peng, Y. *Org. Lett.* **2010**, *12*, 5310.

232

dx.doi.org/10.1021/ja408792k | J. Am. Chem. Soc. 2014, 136, 226−233

(45) Ghorbanian, S.; Tyman, J. H.; Tychopoulos, V. *J. Chem. Technol. Biotechnol.* **2000**, *75*, 1127.

(46) Okazaki, M.; Tanaka, T.; Taniguchi, S. *Yuki Gosei Kagaku Kyokaishi* **1957**, *14*, 344.

(47) Boll, E.; Dheur, J.; Drobecq, H.; Melnyk, O. *Org. Lett.* **2012**, *14*, 2222.

(48) Martin, D. J.; Carl, C. G. *J. Org. Chem.* **1968**, *33*, 1275.

(49) Cui, L.; Zhong, Y.; Zhu, W.; Xu, Y.; Du, Q.; Wang, X.; Qian, X.; Xiao, Y. *Org. Lett.* **2011**, *13*, 928.

(50) Arscott, L. D.; Gromer, S.; Schirmer, R. H.; Becker, K.; Williams, C. H., Jr. *Proc. Natl. Acad. Sci. U.S.A.* **1997**, *94*, 3621.

(51) Javvadi, P.; Hertan, L.; Kosoff, R.; Datta, T.; Kolev, J.; Mick, R.; Tuttle, S. W.; Koumenis, C. *Cancer Res.* **2010**, *70*, 1941.

(52) Rigobello, M. P.; Bindoli, A. *Methods Enzymol.* **2010**, *474*, 109.

(53) Conrad, M.; Schick, J.; Angeli, J. P. *Neurochem. Int.* **2013**, *62*, 738.

(54) Sun, R. W.; Lok, C. N.; Fong, T. T.; Li, C. K.; Yang, Z. F.; Zou, T.; Siu, A. F.; Che, C. M. *Chem. Sci.* **2013**, *4*, 1979.

(55) Klossowski, S.; Muchowicz, A.; Firczuk, M.; Swiech, M.; Redzej, A.; Golab, J.; Ostaszewski, R. *J. Med. Chem.* **2012**, *55*, 55.

(56) Rubbiani, R.; Can, S.; Kitanovic, I.; Alborzinia, H.; Stefanopoulou, M.; Kokoschka, M.; Monchgesang, S.; Sheldrick, W. S.; Wolfl, S.; Ott, I. *J. Med. Chem.* **2011**, *54*, 8646.

(57) Wang, L.; Yang, Z.; Fu, J.; Yin, H.; Xiong, K.; Tan, Q.; Jin, H.; Li, J.; Wang, T.; Tang, W.; Yin, J.; Cai, G.; Liu, M.; Kehr, S.; Becker, K.; Zeng, H. *Free Radicals Biol. Med.* **2012**, *52*, 898.

(58) Schuh, E.; Pfluger, C.; Citta, A.; Folda, A.; Rigobello, M. P.; Bindoli, A.; Casini, A.; Mohr, F. *J. Med. Chem.* **2012**, *55*, 5518.

(59) Arner, E. S.; Nordberg, J.; Holmgren, A. *Biochem. Biophys. Res. Commun.* **1996**, *225*, 268.

(60) Shay, K. P.; Moreau, R. F.; Smith, E. J.; Smith, A. R.; Hagen, T. M. *Biochim. Biophys. Acta* **2009**, *1790*, 1149.

(61) Sanadi, D. R.; Langley, M.; Searls, R. L. *J. Biol. Chem.* **1959**, *234*, 178.

(62) Cheng, Z.; Arscott, L. D.; Ballou, D. P.; Williams, C. H., Jr. *Biochemistry* **2007**, *46*, 7875.

(63) Besse, D.; Siedler, F.; Diercks, T.; Kessler, H.; Moroder, L. *Angew. Chem., Int. Ed. Engl.* **1997**, *36*, 883.

(64) Rost, J.; Rapoport, S. *Nature* **1964**, *201*, 185.

(65) Chan, J.; Dodani, S. C.; Chang, C. J. *Nat. Chem.* **2012**, *4*, 973.

(66) Arner, E. S.; Sarioglu, H.; Lottspeich, F.; Holmgren, A.; Bock, A. *J. Mol. Biol.* **1999**, *292*, 1003.

(67) Zhong, L.; Holmgren, A. *J. Biol. Chem.* **2000**, *275*, 18121.

(68) Levanova, E. P.; Grabel'nykh, V. A.; Sukhomazova, E. N.; Zemirova, I. A.; Russavskaya, N. V.; Albanov, A. I.; Klyba, L. V.; Zhanchipova, E. R.; Korchevin, N. A. *Russ. J. Org. Chem.* **2008**, *44*, 1428.